

NATIONAL ADVISORY COMMITTEE FOR AERONAUTICS

RESEARCH MEMORANDUMLATERAL-CONTROL CHARACTERISTICS AND DIHEDRAL EFFECT OF A WING-BODY
COMBINATION WITH A VARIABLE-INCIDENCE TRIANGULAR WING AND
WING-TIP AILERONS AT A MACH NUMBER OF 1.52

By Richard Scherrer and David H. Dennis

SUMMARY

Aileron effectiveness and dihedral effect were investigated for a wing-body combination having a variable-incidence triangular wing with modified half-delta controls at the wing tips. The tests were conducted at a Mach number of 1.52 at a Reynolds number of 0.82 million. At the Mach number of the tests, the Mach cone from the wing apex was almost coincident with the wing leading edge.

The experimental value of aileron effectiveness at 0° angle of attack was approximately 78 percent of the value predicted by linear theory, and the effectiveness decreased with increasing wing angle of attack. The theoretical effectiveness of the modified half-delta ailerons was compared with that of half-delta wing-tip ailerons, and the half-delta design was found to be slightly more effective. The rolling-moment data obtained in the dihedral-effect tests indicated that the wing-body combination was unstable at small angles of sideslip at the maximum angle of incidence tested.

INTRODUCTION

Research on lateral-control devices for supersonic aircraft with low-aspect-ratio wings has indicated that the conventional trailing-edge-flap control surface loses much of its effectiveness at transonic and supersonic speeds. (See reference 1.) This loss in effectiveness has been found to result primarily from the nature of the boundary-layer flow over the rear part of the wing. As a result, research on lateral-control devices has been directed toward the investigation of other control configurations. Controls placed at the wing tips have been found to be satisfactory, particularly for low-aspect-ratio wings of triangular plan form. (See references 1, 2, and 3.)

For all the ailerons considered in this report, the control surface consists of a portion of the tip of a wing of triangular plan form; the

edge between the wing and the control surface is parallel to the air stream; and the hinge line is perpendicular to this edge. As shown in reference 4, deflection of ailerons of this type in supersonic flow induces lift on the adjacent wing surface. This induced lift, together with the greater moment arm about the roll axis and better boundary-layer flow, causes this type of aileron to be more effective than the trailing-edge type.

The first phase of the present investigation was undertaken to determine the effectiveness, at a Mach number of 1.52, of a triangular wing-tip aileron with a raked-in trailing edge. The trailing edge was located approximately along the Mach line extending forward from the point of intersection of the wing trailing edge and the aileron root chord. Another part of this phase of the investigation consisted of the comparison of the experimental results with the theoretical effectiveness of the test ailerons in order to determine the agreement between theory and experiment when the wing leading edge and bow wave are almost coincident. In addition, the theoretical effectiveness of the test ailerons was compared with the theoretical effectiveness of half-delta ailerons of equal size.

The wing-aileron combination of the present investigation was intended for use in a guided-missile design with a variable-incidence wing. Since no data were available on the effect of wing incidence on the rolling moment due to sideslip of a variable-incidence wing in combination with a slender body, this characteristic was investigated as a second phase of the test program.

The tests were conducted at the request of the U. S. Air Force. The model and strain-gage balance were furnished by the Boeing Airplane Company.

SYMBOLS

b	wing span, 4.74 inches
\bar{c}	mean aerodynamic chord, 1.86 inches
S	total wing area (including that within the body), 8.78 square inches
V	free-stream velocity, feet per second
q	free-stream dynamic pressure, pounds per square inch
L	rolling moment about body longitudinal axis, inch pounds (Positive moments are clockwise when the aircraft is viewed from the rear.)
C_l	rolling-moment coefficient $\left(\frac{L}{qSb} \right)$, dimensionless

$\Delta C_{l\delta_a}$	increment of rolling-moment coefficient due to aileron deflection, dimensionless
M_0	free-stream Mach number, dimensionless
p	rate of roll, radians per second
Re	Reynolds number based on the mean aerodynamic chord of the wing, dimensionless
α	angle of attack of the body, degrees
i	angle of wing incidence measured from the body axis to the wing-chord plane, degrees
δ_a	aileron deflection angle measured from the wing-chord plane to the aileron chord plane, degrees (Positive deflections produce positive lift.)
β	angle of sideslip measured from body axis to the free-stream direction, degrees (Positive angles are with the nose to the left when viewed from from the rear.)
$\frac{pb}{2V}$	wing-tip helix angle, radians
μ	Mach angle, 41.1° at test Mach number
ϵ	wing semi-apex angle, 40.5°

APPARATUS

The experiments were performed in the Ames 1- by 3-foot supersonic wind tunnel No. 1. This closed-circuit variable-density wind tunnel is equipped with a nozzle having flexible top and bottom plates which can be shaped to give test-section Mach numbers between 1.2 and 2.4. The absolute total pressure in the wind tunnel can be varied from one-fifth of an atmosphere to three atmospheres, depending on the Mach number and ambient air temperature. The air in the wind tunnel is dried to an absolute humidity of 0.0001 pound of water per pound of dry air in order to make the effects of condensation in the nozzle negligible. For the present investigation, the model was mounted on a sting support attached to the wind-tunnel balance housing. The angle of attack was varied by pitching the model, sting, and balance housing about a point at the rear of the housing. With this arrangement, the model moved vertically in passing through the angle-of-attack range and was located on the longitudinal axis of the wind tunnel at zero angle of attack. A photograph of the model mounted in the test section is shown in figure 1.

A drawing of the wing-body combination that was employed in the investigation is shown in figure 2, and the dimensions and areas of the wing and ailerons are given in figure 3. The aileron trailing edges were raked in at an angle such that the trailing edges were slightly within the Mach cone from the tip of the aileron. A photograph of all the components of the model is shown in figure 4. The model was designed so that nominal wing-incidence angles of 0° , 6° , 10° , and 15° could be obtained. Nominal aileron angles of 0° , 10° , and 15° were obtained by using separate pairs of ailerons for each angle.

The airfoil section was flat-sided with wedge-shaped leading and trailing edges and the wing thickness-to-chord ratio varied from 0.048 at the root to 0.087 at the aileron root-chord line. The body had a small hemispherical tip which was faired into the cylindrical portion by an ogival section. The model assembly was held together by the ogival nose which screwed onto the center body. The model design allowed rapid and accurate changes to be made in the model configuration.

The balance used to measure the forces acting on the model was located as shown in figure 2 and was an integral part of the support sting. The rolling moment about the model axis was measured with electrical resistance strain gages located on small vertical beams within the balance.

TESTS

All the tests of the present investigation were conducted with the one wing-body combination at a Mach number of 1.52 and at a total pressure of 18 pounds per square inch absolute. The Reynolds number of the tests, based on the mean aerodynamic chord of the wing, was 0.82 million. Other test conditions for both phases of the investigation are given in the following table:

Test	Aileron effectiveness	Dihedral effect
δ_a	$0^\circ, 10^\circ, 15^\circ$	0°
i	$0^\circ, 6^\circ, 10.3^\circ, 15.2^\circ$	$0^\circ, 6^\circ, 10.3^\circ, 15.2^\circ$
α	-2° to $+5.5^\circ$	0°
β	0°	-2° to $+5.5^\circ$

The aileron-effectiveness tests were made with the spanwise axis of the model placed horizontally as shown in figure 1, and the dihedral-effect tests were made with the model rotated 90° on the balance so that the spanwise axis was in a vertical plane.

The effects of the small stream angles and static pressure variations which exist in the wind tunnel were eliminated from the plotted data in the aileron-effectiveness tests by considering only the increment of rolling-moment coefficient due to aileron deflection at each wing angle of attack ($\alpha+i$). These effects could not be eliminated completely in the dihedral-effect tests by considering the rolling-moment coefficients due to incremental changes in wing incidence because the wing was much larger relative to the stream irregularities than the ailerons and therefore the effects of these irregularities could be expected to change slightly with wing incidence. Consequently, the results from the dihedral-effect tests could not be presented in incremental form. The measured values of angle of attack and sideslip have been corrected for the effect of sting deflection caused by aerodynamic loads by means of a calibration factor obtained with static loads just prior to the tests. Estimates of the errors in measurement to be expected in each of the variables entering into the presentation of the data are given in the following table:

Variable	Error	Variable	Error
α	$\pm 0.2^\circ$	C_l	± 0.0001
i	$\pm 0.2^\circ$	M	± 0.01
δ	$\pm 0.5^\circ$	Re	$\pm 20,000$
β	$\pm 0.2^\circ$	---	---

It should be noted that, although the accuracy to which the rolling-moment coefficient could be measured was 0.0001, the possible error in aileron-angle setting could cause a constant error of several times this value. When the aileron angles were large (aileron-effectiveness tests) the total percent accuracy was good, but when the nominal aileron angle was zero, as in the dihedral-effect tests, the effect of the error in the aileron setting on the percent accuracy became large.

RESULTS AND DISCUSSION

Aileron Effectiveness

The variation, with angle of attack of the wing, of the increment of rolling-moment coefficient due to aileron deflection is shown in figure 5. For wing angles of attack ($\alpha+i$) up to 14° the data for all angles of incidence plot as almost a single curve; therefore, the increments of rolling-moment coefficient are independent of body angle of attack α in the test range. At high angles of attack of the wing (above 14°) the

rolling-moment data become erratic. Since this change in the curves occurs at almost the same angle of attack at both aileron angles (10° and 15°), it probably originates from some change in the flow on the wing rather than on the ailerons.

As shown in figure 5 the values of the rolling-moment coefficients decrease by almost one-third from a wing angle of attack of 0° to an angle of 14° . Because of this effect and because of the erratic results at high angles of attack, a test was made using the liquid-film technique described in reference 5 in order to visualize the flow in the boundary layer. The model was installed at a body angle of attack of 0° with a wing-incidence angle of 15.2° and aileron angles of $\pm 15^\circ$. The liquid-film pattern indicated that separation of the flow occurred over the aileron with the higher angle of attack and over the upper surface of the wing adjacent to this aileron in the region aft of the pressure wave from the forward tip of the aileron. The pattern also indicated that the boundary layer flowed from the high- to the low-pressure regions through the gaps between the wing and ailerons. These results indicate that the decrease in aileron effectiveness and the erratic rolling-moment data obtained at wing angles of attack ($\alpha+i$) above 14° may be attributable to the effects of the wing-aileron gaps and flow separation at high aileron angles of attack ($\alpha+i+\delta_a$).

The change in rolling-moment coefficient with aileron deflection, determined by the theory of reference 4, is 0.00115 per degree aileron deflection. The corresponding experimental value at zero wing incidence and zero aileron angle, as determined from a cross plot of the data in figure 5, is approximately 0.0009, or about 78 percent of the theoretical value. This percentage agreement between theory and experiment is similar to that reported in references 2 and 3.

In order to compare the effectiveness of the test aileron with that of another similar type on the same basic wing, the effectiveness of a half-delta wing-tip aileron of the same area relative to the wing was calculated. The theoretical effectiveness of this aileron ($\partial C_l / \partial \delta_a$) was found to be 0.00125, or about 9 percent greater than that of the ailerons with raked-in-tips. Because the damping-in-roll derivative, $\frac{\partial C_l}{\partial (pb/2V)}$, of the test wing can be expected to be almost the same as that of the triangular wing with half-delta ailerons, because the differences in wing area and span are small, the difference between the values of the rolling-effectiveness parameter, $\frac{\partial (pb/2V)}{\partial \delta_a}$, should also be about 9 percent. In addition to being slightly less effective, the test ailerons can be expected to have less desirable hinge-moment characteristics than half-delta ailerons at Mach numbers below 1.5 because of the decrease in lift in the area behind the Mach wave from the wing tip.

An interesting point in the comparison of half-delta ailerons and the ailerons with raked-in tips is that in the latter case, according to linearized theory, 40 percent of the lift was carried on the wing, while in the former case only 18 percent of the lift was carried on the wing. The fact that the average loading on the modified half-delta aileron is less than that on a half-delta aileron counteracts the effect of the increased lift carry-over of the former, with the result that the final values of aileron effectiveness are not markedly different.

Dihedral Effect

The effect of wing incidence on the rolling-moment coefficient due to sideslip with zero aileron deflection and zero angle of attack are shown in figure 6. The vertical displacement from the horizontal axis of the curve for zero wing incidence is indicative of the displacement that can be expected in any of the other curves of figure 6. The average value of this displacement (0.0005) is equivalent to an aileron deflection of 0.6° which is approximately equal to the estimated accuracy of the aileron settings ($\pm 0.5^\circ$). Since an error in aileron setting could only cause an almost constant displacement of the curve for zero incidence in figure 6, the variations in the curve must result from some other effect. A vertical variation of lateral stream angle in the wind tunnel could result in such an effect and this is believed to be the case in the present experiments. The uncertainty in the slopes of the curves of figure 6 is believed to be of the order of the slopes of the curve for zero wing incidence. With this degree of uncertainty, the data are inconclusive in regard to the stability of the configuration wherever the slopes are small.

The slopes of the curves for incidence angles of 6° , 10.3° , and 15.2° at large angles of sideslip indicate positive stability, but the curve for 15.2° at small angles of sideslip indicates negative stability. It is concluded, therefore, that the configuration tested can be expected to be laterally unstable at small angles of sideslip at high angles of incidence. The effect of sideslip on the rolling moment of triangular wings has been investigated theoretically (see reference 6), and the theory indicates that with the present wing a change in the sign of the

dihedral effect $\left[\frac{d(C_l/\alpha)}{d\beta} \right]$ occurs at Mach numbers at which the Mach

cone crosses the wing leading edge. However, the theory, which is limited to small angles, does not indicate any change in sign with increasing wing angle of attack. The present experiments were not sufficiently detailed to indicate the cause of the lateral instability and further research is required before the cause can be determined.

CONCLUSIONS

The results of theoretical calculations and wind-tunnel tests of a wing-body combination having a variable-incidence triangular wing and modified, half-delta, wing-tip controls at a Mach number of 1.52 lead to the following conclusions:

1. The experimental value of aileron effectiveness ($\partial C_l / \partial \delta_a$) at 0° angle of attack was approximately 78 percent of that predicted by linearized theory, and the effectiveness decreased with increasing wing angle of attack.
2. The wing-body combination was found to be laterally unstable at small angles of sideslip at the maximum test angle of wing incidence (15.2°).
3. The theoretical calculations indicate that the half-delta wing-tip controls with raked-in tips have slightly less rolling effectiveness near the design Mach number than full half-delta controls of the same area on a triangular plan-form wing.

Ames Aeronautical Laboratory,
National Advisory Committee for Aeronautics,
Moffett Field, Calif.

REFERENCES

1. Sandahl, Carl A., and Strass, H. Kurt: Comparative Tests of Rolling Effectiveness of Constant-Chord, Full-Delta, and Half-Delta Ailerons on Delta Wings at Transonic and Supersonic Speeds. NACA RM L9J26, 1949.
2. Conner, D. William, and May, Ellery B., Jr.: Control Effectiveness and Hinge-Moment Characteristics of a Tip Control Surface on a Low-Aspect-Ratio Pointed Wing at a Mach Number of 1.9. NACA RM L9H26, 1949.
3. Conner, D. William, and May, Ellery B., Jr.: Control Effectiveness, Load and Hinge-Moment Characteristics of a Tip Control Surface on a Delta Wing at a Mach Number of 1.9. NACA RM L9H05, 1949.
4. Lagerstrom, P. A., and Graham, Martha E.: Linearized Theory of Supersonic Control Surfaces. Jour. Aero. Sci., vol. 16, no. 1, Jan. 1949, pp. 31-34.
5. Vincenti, Walter G., Nielsen, Jack N., and Matteson, Frederick H.: Investigation of Wing Characteristics at a Mach Number of 1.53. I - Triangular Wings of Aspect Ratio 2. NACA RM A7I10, 1947.
6. Jones, Arthur L., Spreiter, John R., and Alksne, Alberta: The Rolling Moment Due to Sideslip of Triangular, Trapezoidal and Related Plan Forms in Supersonic Flow. NACA TN 1700, 1948.

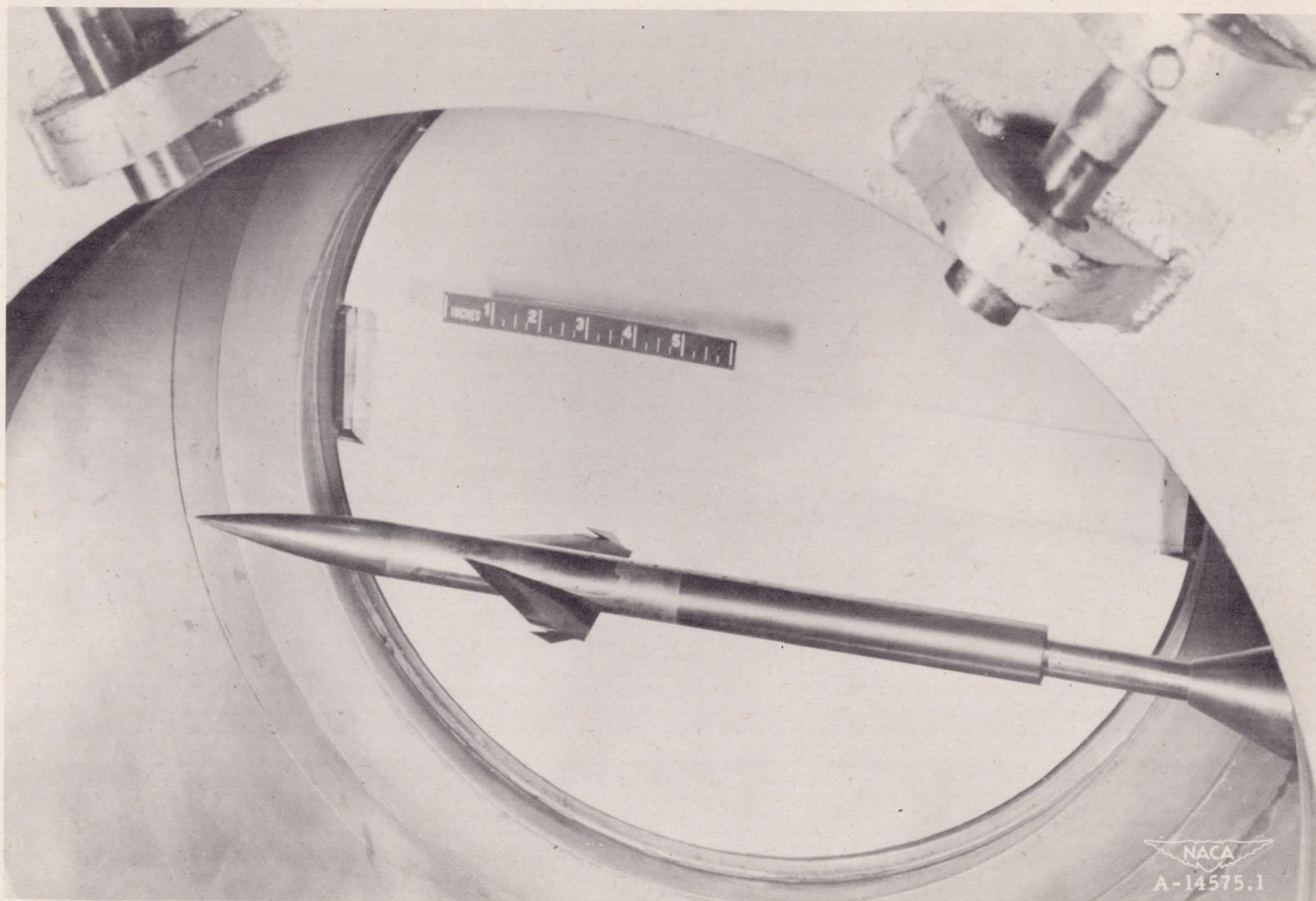


Figure 1.- Wing-body combination installed in the Ames 1-by 3-foot supersonic wind tunnel No. 1; $i = 10^\circ$, $\delta = \pm 15^\circ$.

03112301040

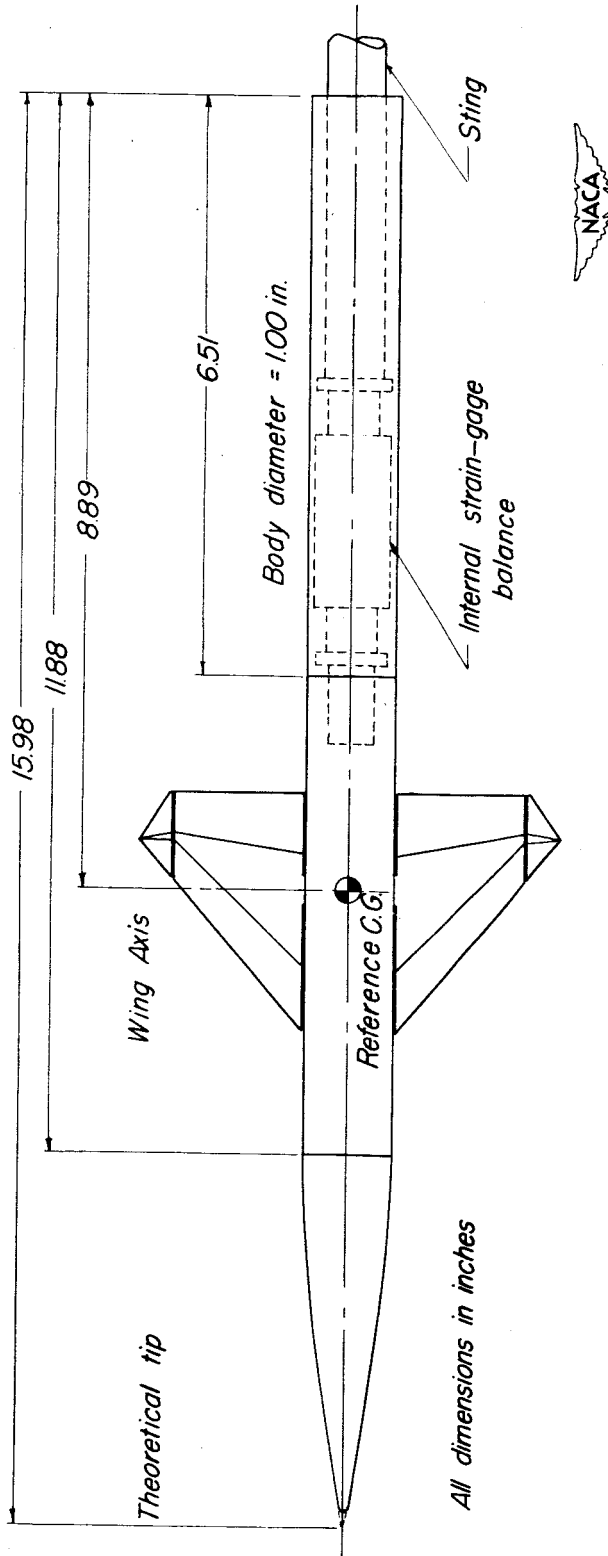
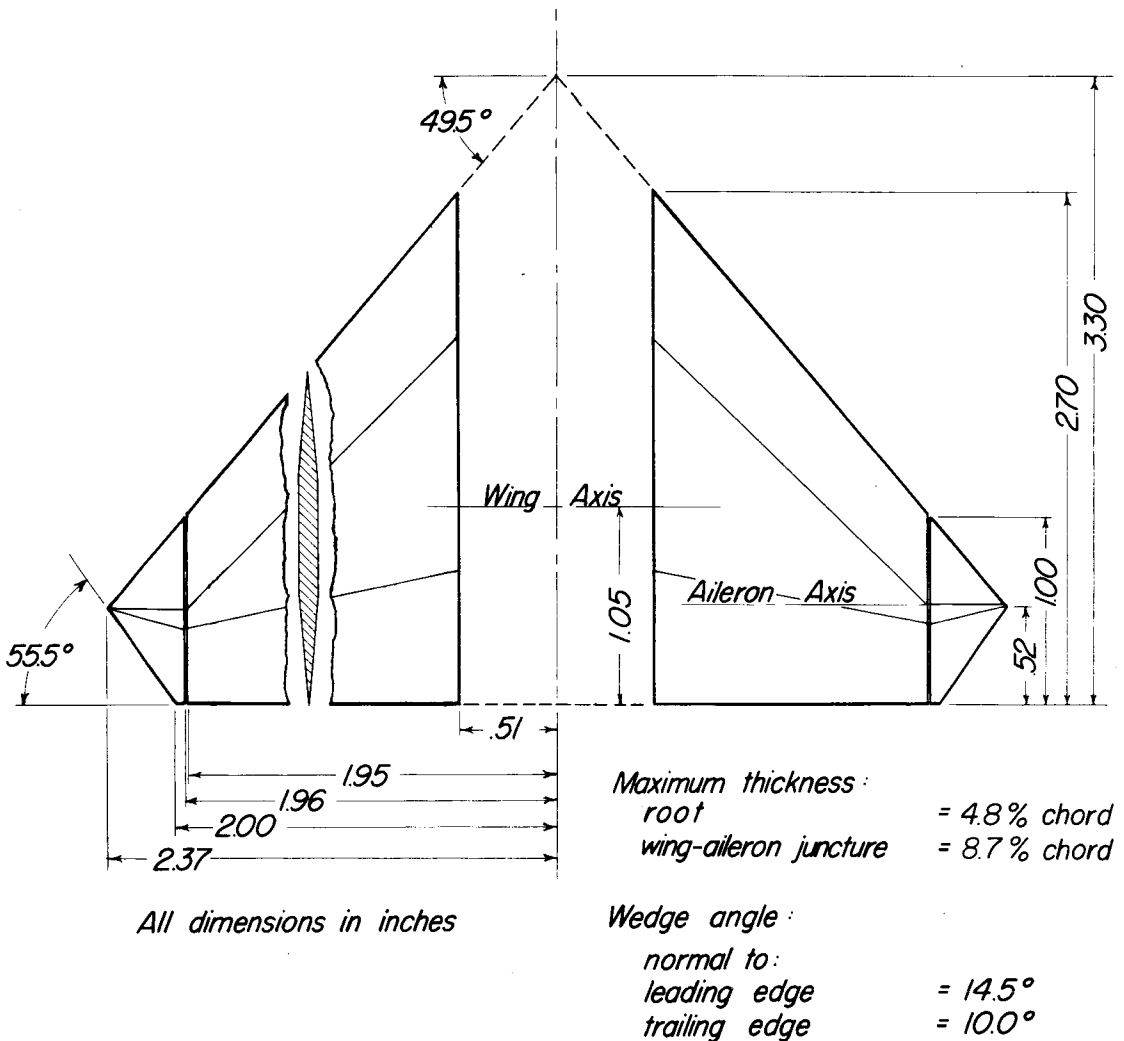


Figure 2.- Plan view of wing-body combination showing the relative positions of the wing and strain-gage balance.

Exposed Wing Area = 5.72 in.²
 Total Wing Area = 8.78 in.²
 Aspect Ratio = 2.55
 Aileron Area = .21 in.² (each)



All dimensions in inches



Figure 3. — Dimensions and areas of the wing and ailerons.

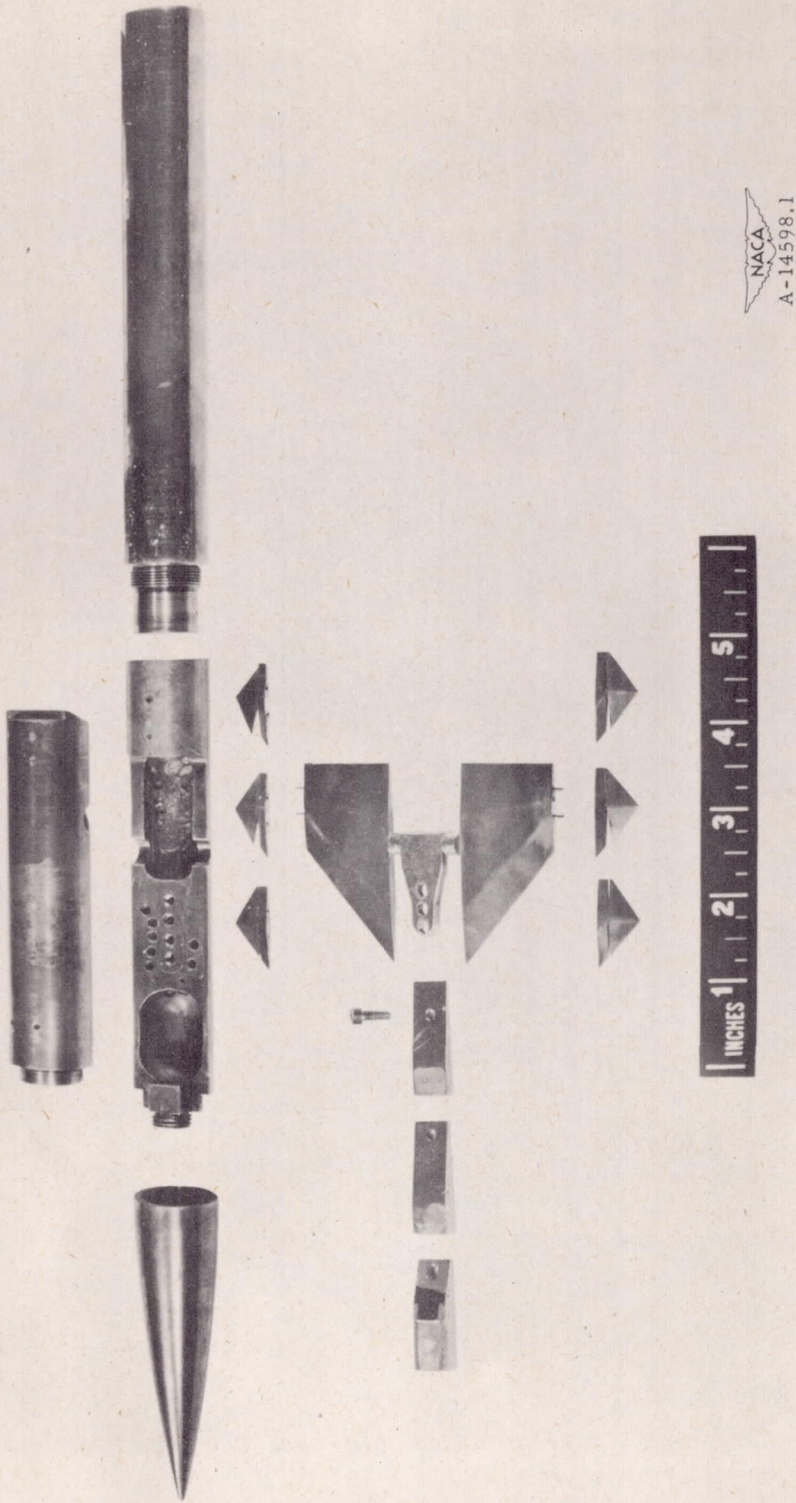


Figure 4.- Components of the wing-body combination.

0317122A J04U

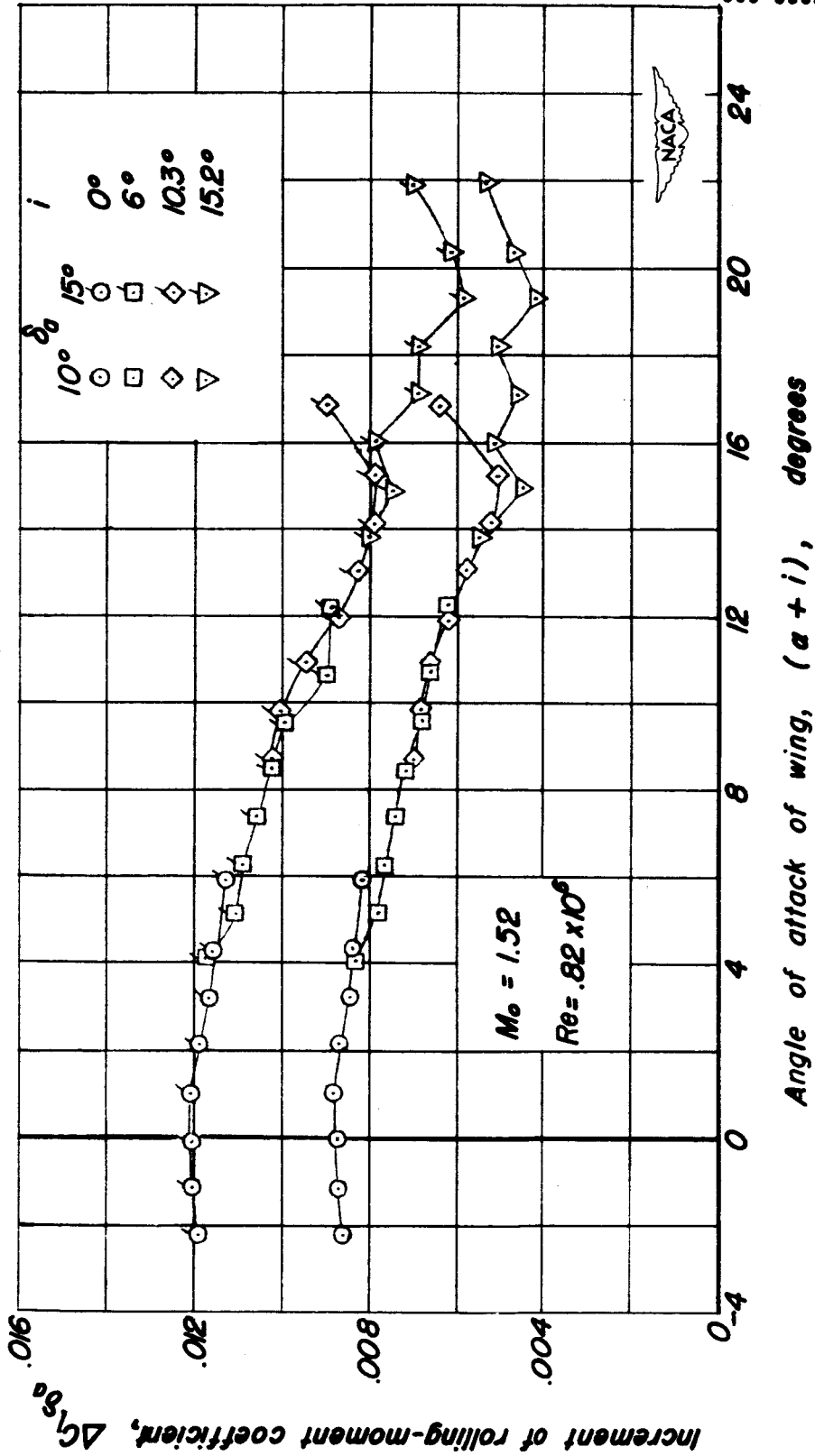


Figure 5. — The variation of the increment of rolling-moment coefficient due to aileron deflection with angle of attack of the wing.

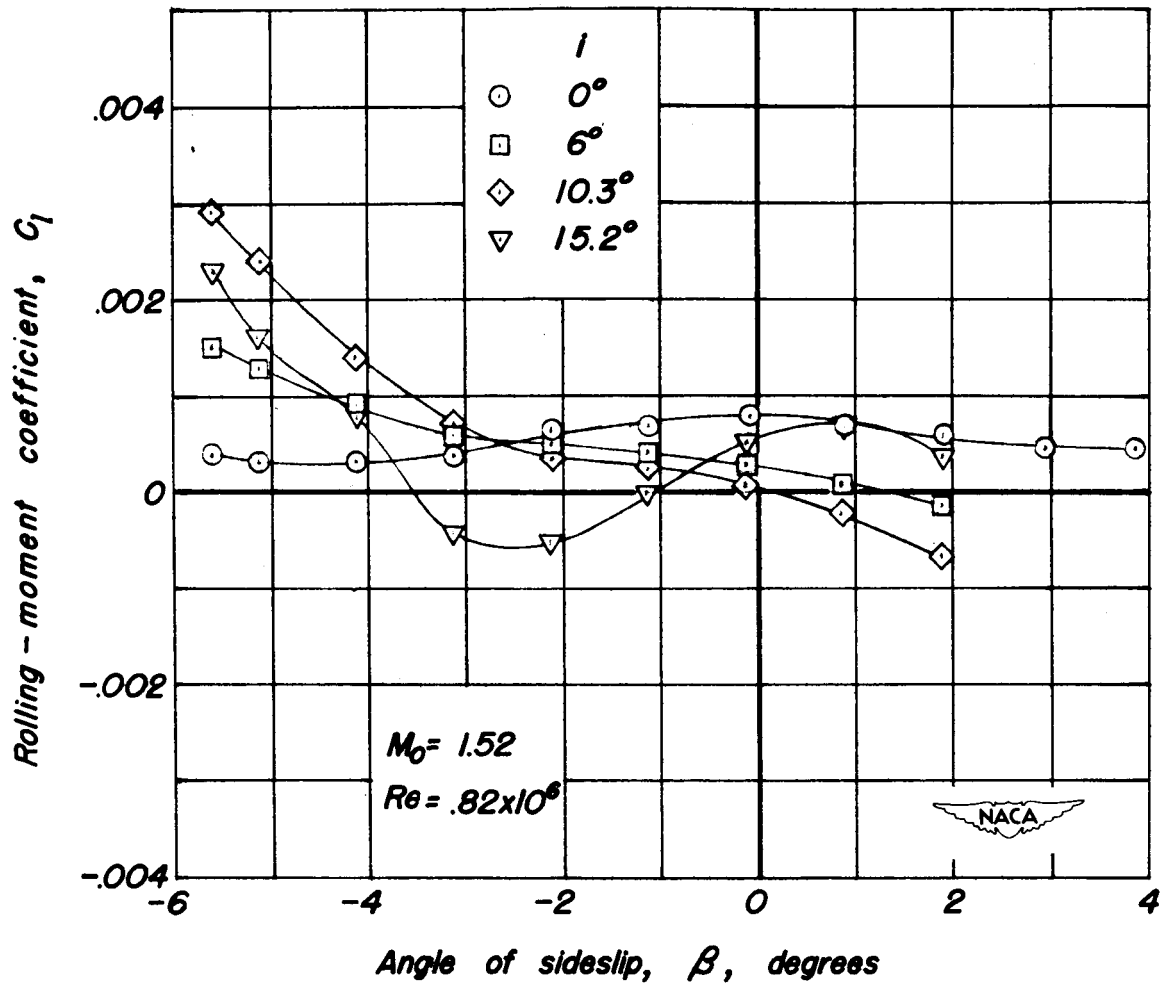


Figure 6. — The variation of rolling-moment coefficient with angle of sideslip at several angles of wing incidence, $\alpha = 0^\circ$; $\delta_a = 0^\circ$.

Code 1

031712301040

copy #1

UNCLASSIFIED